catalysts

MDPI

Article

Green Synthesis of Zinc Oxide Nanoparticles Using *Nostoc* sp. and Their Multiple Biomedical Properties

Lubna Anjum Minhas [1], Abdul Samad Mumtaz [1,*], Muhammad Kaleem [1], Dunia Al Farraj [2], Khalid Kamal [3], Malik Aamer Hassan Minhas [4], Rooma Waqar [1,5] and Rania M. Mahmoud [5]

[1] Department of Plant Sciences, Faculty of Biological Sciences, Quaid-i-Azam University, Islamabad 45320, Pakistan
[2] Department of Botany and Microbiology, College of Science, King Saud University, P.O. Box 2455, Riyadh 11451, Saudi Arabia
[3] Department of Chemistry, Faculty of Chemical Science, Kohat University of Science and Technology, Kohat 26000, Pakistan
[4] Department of General Management, University of Wales Trinity St David, London SW9 6EJ, UK
[5] Department of Botany, Faculty of Science, University of Fayoum, Fayoum 63514, Egypt
* Correspondence: asmumtaz@qau.edu.pk

Abstract: Zinc oxide nanoparticles (ZnONPs) are the top candidate in the field of biological applications because of their high surface area and excellent catalytic activities. In the present study, the cyanobacteria-mediated biosynthesis of zinc oxide NPs using *Nostoc* sp. extract as a stabilizing, chelating, and reducing agent is reported. ZnONPs were biologically synthesized using an eco-friendly and simple technique with a minimal reaction time and calcination temperature. Various methods, including X-ray diffraction (XRD), ultraviolet spectroscopy (UV), Fourier transform infrared (FTIR), scanning electron microscopy (SEM), and energy-dispersive X-ray spectroscopy (EDX) were used to characterize the biosynthesized zinc oxide NPs. XRD analysis depicted the crystalline form of zinc oxide NPs, and the Scherrer equation determined a mean crystalline size of ~28.21 nm. The SEM results reveal the spherical shape of the biosynthesized nanoparticles. Various functional groups were involved in the capping and stabilization of the zinc oxide NPs, which were confirmed by FTIR analysis. The zinc oxide NPs showed strong UV-vis absorption at 340 nm. Multiple in vitro biological applications showed significant therapeutic potential for zinc oxide NPs. Potential antimicrobial assays were reported for zinc oxide NPs via the disc-diffusion method and food poisoning method, respectively. All other activities mentioned below are described with the concentration and IC50 values. Biocompatibility with human erythrocytes and macrophages (IC50: 433 µg/mL, IC50 > 323 µg/mL) and cytotoxic properties using brine shrimps (IC50: 11.15 µg/mL) and *Leishmania tropics* (Amastigotes IC50: 43.14 µg mL^{-1} and Promastigotes IC50: 14.02 µg mL^{-1}) were determined. Enzyme inhibition assays (protein kinase and alpha amylase) were performed and showed strong potential. Free radical scavenging tests showed strong antioxidant capacities. These results indicate that zinc oxide NPs synthesized by *Nostoc* sp. have strong biological applications and are promising candidates for clinical development.

Keywords: *Nostoc* sp.; zinc oxide NPs; characterization; biological applications; green synthesis

check for updates

Citation: Minhas, L.A.; Mumtaz, A.S.; Kaleem, M.; Farraj, D.A.; Kamal, K.; Minhas, M.A.H.; Waqar, R.; Mahmoud, R.M. Green Synthesis of Zinc Oxide Nanoparticles Using *Nostoc* sp. and Their Multiple Biomedical Properties. *Catalysts* **2023**, *13*, 549. https://doi.org/10.3390/catal13030549

Academic Editors: María Eugenia Rabanal Jiménez, Paloma Fernández Sánchez and Ana Urbieta

Received: 5 January 2023
Revised: 24 February 2023
Accepted: 3 March 2023
Published: 9 March 2023

Copyright: © 2023 by the authors. Licensee MDPI, Basel, Switzerland. This article is an open access article distributed under the terms and conditions of the Creative Commons Attribution (CC BY) license (https://creativecommons.org/licenses/by/4.0/).

1. Introduction

Nanotechnology has grown significantly due to its usage in biotechnology, chemistry, and pharmacology [1,2]. As a result of this research, particular innovations in drug delivery, gene transport, nanomedicine, biosensing, and other aspects of nanoscience have been developed [3,4]. One of the unique characteristics of nanotechnology that makes nano-sized particles exciting is their high surface-to-volume ratio [5]. Atoms present on the surface are more active than those present on the inner side of nanoparticles. This property of nanoparticles makes them more reactive than bulk materials [6]. Nanoparticles can be

synthesized by chemical, physical, or biological methods. Different chemical and physical methods, including laser ablation, hydrothermal, sol-gel synthesis, lithography, and others, require special equipment and skilled people. Additionally, they affect human health negatively. In contrast, the biological methods used for the synthesis of nanoparticles are inexpensive, nontoxic, and biodegradable [7–10]. The utilization of natural resources, including leaves, roots, and flower extracts, as well as microorganisms such as bacteria, fungus, and algae, etc., are eco-friendly methods of NPs synthesis that use fewer toxic compounds [11–13]. Recently, more importance has been given to the biosynthesis of metal oxide nanoparticles, including gold, copper, zinc, silver, and nickel nanoparticles [14–16].

There are various chemical, biological, and physical methods for synthesizing zinc oxide NPs. According to the literature, the chemical methods used to synthesize zinc oxide nanoparticles include wet chemical, electro-deposition, chemical micro-emulsion, spray pyrolysis, [17], microwave-assisted combustion, and chemical and direct precipitation. Physical methods include high vacuum usage in processes such as thermal evaporation, pulsed laser deposition, and molecular beam epitaxy [18]. Among these, the biological methods are eco-friendly and cost-effective for the fabrication of zinc oxide nanoparticles [19]. In "green synthesis", plant extracts, fungi, bacteria, and microorganisms are used to synthesize zinc oxide nanoparticles (ZnONPs) [20].

Among all other microorganisms, cyanobacteria are of particular interest in the biosynthesis of nanoparticles because they are a potential source of novel compounds, with great biotechnological value [21,22]. Compared to crop plants, cyanobacterial culture and biomass production systems require significantly less time to grow and have maximum biomass capacity [23]. Pd, Ag, Au, and Pt nanoparticles have been synthesized using cyanobacteria either extracellularly or intracellularly [24]. EA03 and *Arthrospira platensis* have also been used to synthesize ZnONPs [21,25].

The primary benefit is the possibility for biosynthesized nanoparticles to be used in biomedical applications or directly in living systems. This is because these nanoparticles have a lower degree of toxicity than those made via physicochemical processes. Pillai et al. reported the antibacterial and antifungal activities of zinc oxide nanoparticles synthesized from aqueous extract of plants [26]. The genus *Nostoc* is a rich source of a variety of secondary metabolites, including vitamins, phycobiliproteins, antioxidants, enzymes, and phenolic compounds, which are often used as anticancer, anti-HIV, antimalarial, antifungal, or antibacterial [27] medicines [28]. *Nostoc* cell extract can be used as a metal oxide coating and reducing agent for the NP synthesis of NPs, as it is a rich source of compounds such as amino, hydroxyl, and carboxyl groups [29].

The main objectives of this study were to use *Nostoc* sp. biomass for the biosynthesis of zinc oxide nanoparticles to ensure environmentally friendly formation, reduce toxic precursors and by-products, and determine if they are safe and effective in treating emerging diseases. The present study investigated the synthesis of safe and secure metal oxide NPs. The potential of *Nostoc* sp. extract in the production of highly crystalline, pure zinc oxide NPs were evaluated, along with their structural, thermal, and optical properties. Zinc oxide NPs were also evaluated for their antifungal, antibacterial, and cytotoxicity properties in brine shrimps and *Leishmania tropica*, their biocompatibility with human RBC (red blood cells) and macrophages, their enzyme inhibition potential by protein kinase (PK) and α-amylase (AA), and their antioxidant capacities. The results provide detailed information about biosynthesis and, the suitability of zinc oxide NPs for biological activities is discussed.

2. Results and Discussion

2.1. Physical and Chemical Characterization of Green-Synthesized Zinc Oxide Nanoparticles

2.1.1. UV-Vis Spectrum

In this study, the cyanobacterial extract of *Nostoc* sp. was utilized to biosynthesize zinc oxide NPs, which act as stabilizing and reducing agents. Progress in the development of zinc oxide NPs was carried out through different characterization techniques. The

formation of biosynthesized zinc oxide NPs was confirmed by a color change after the addition of zinc acetate to the cyanobacterial extract at 60 °C. The color change from dark green to turbid white was due to surface plasmon resonance [30]. To monitor the stability of zinc oxide NPs, 1 mg mL^{-1} solutions of zinc oxide NPs were prepared and sonicated for 40 min. After 48 h, the turbid colloidal solution was left to stabilize, and the surface plasmon resonance was detected at various time periods. The solution was scanned over the specified wavelength scale of 200–800 nm. The UV spectra revealed an absorption peak at 340 nm, indicating the stability of the colloidal solution at 48 h. After 60 h, there was a reduction in the absorption peak, indicating that the NPs had settled down. Figure 1A,B represents the UV-vis spectrum of the biosynthesized Nostoc-mediated zinc oxide nanoparticles.

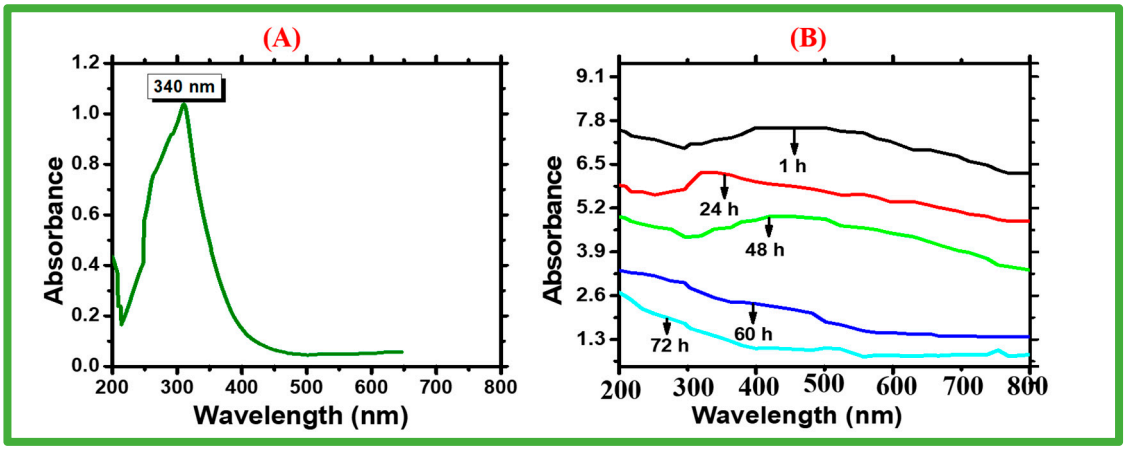


Figure 1. UV-vis spectra analysis of biosynthesized zinc oxide NPs. (**A**) UV-vis spectra, and (**B**) stability of green-synthesized zinc oxide NPs.

2.1.2. FTIR Spectroscopy

The chemical structures and functional groups of the biosynthesized zinc oxide nanoparticles using Nostoc sp. were determined by FTIR spectroscopy (Figure 2). The results of the FTIR spectroscopy show seven intense peaks at 3535 cm^{-1}, 3020 cm^{-1}, 1600 cm^{-1}, 1157 cm^{-1}, 1025 cm^{-1}, 449 cm^{-1}, and 684 cm^{-1}. The broad absorption peaks at 3535 cm^{-1} indicate the presence of O-H hydrogen bands [31]. It is possible that intra-and inter-molecular hydrogen bonding formation contributed to the width of this peak [32]. While the band at 1600 cm^{-1} was associated with the C=O stretching of proteins (Jabs 2005) or residual acetate, the low-intensity peak at 3000 cm^{-1} was associated with the CH_2 stretching of asymmetric and symmetric carbohydrates or lipids [33]. The vibrational bending at wavenumber 3020 cm^{-1} was caused by the absorption waves of the CH_2 or CH_3 of proteins [32]. The observed band at a wavelength of 1025 cm^{-1} can be attributed to the C-O-C ether of polysaccharides, and the band at a wavelength of 1175 cm^{-1} corresponds to the C-N stretch of amino acids [34]. The absorption band at 449 cm^{-1} proves that Zn-O was formed successfully. In agreement with our data, the FTIR spectroscopy results of the biosynthesized zinc oxide nanoparticles show that zinc oxide absorption bands at wavelengths of 485 cm^{-1} [35] and 442 cm^{-1} [36] were observed in the range 400 to 500 cm^{-1} [37], or at wavelengths of 782 cm^{-1} [38], 450 cm^{-1}, and 600 cm^{-1} [39]. The results of the FTIR spectroscopy show that the extract of *Nostoc* sp. contains organic substances that act as stabilizing, capping, and reducing agents for the biosynthesis of zinc oxide nanoparticles. According to Azizi et al. [40], the interaction between zinc molecules in salt precursors and oxygen-containing functional groups in *Sargassum muticum* cell extract led to the biosynthesis of zinc oxide NPs.

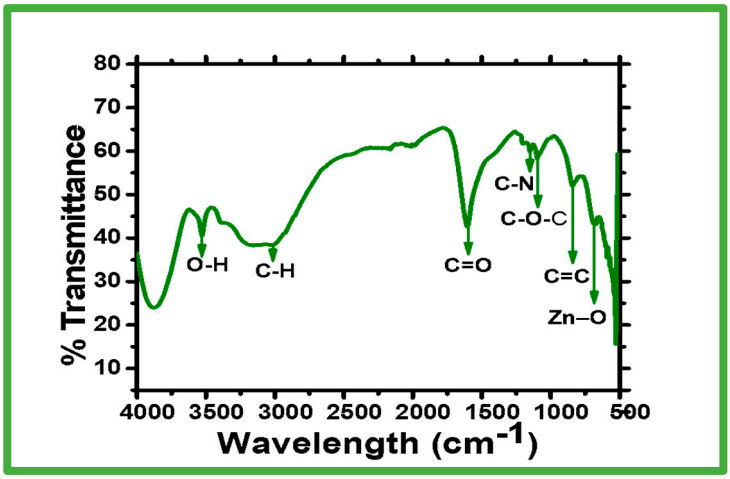


Figure 2. FTIR spectra of green-synthesized ZnONPs.

2.1.3. SEM and EDX

The shape and morphology of biogenic zinc oxide nanoparticles were determined by SEM imagery. The shape of the zinc oxide NPs was spherical or agglomerated, and the SEM images are shown in Figure 3A. The EDX spectrum confirms the quantitative elemental structure of the biosynthesized zinc oxide NPs, as shown in Figure 3B. The data analysis determined that the biosynthesized zinc oxide NPs were composed of Zn, Na, Al, O, and C, with weight percentages of 58.6, 21.3, 13.4, 4.5, 15.3, 4.5, and 3.2%, respectively. The EDX spectrum shows that zinc oxide was successfully produced using the metabolites present in the *Nostoc* sp. filtrate. In addition, the EDX spectrum confirms that Zn and O accounted for the majority of the components of the nanostructure. The involvement of capping agents, such as amino acids, sugar, proteins, and polysaccharides, which are considered the principal constituents of algal extract according to their X-ray emission spectra, can be the source of additional peaks, such as C, Na, and Al, and all of these are in line with previously reported results [41]. According to a recent study, Zn and O account for the majority of zinc oxide NPs biosynthesized by the cyanobacterium *Nostoc* sp. [21]. In addition, Zn and O have been identified as the primary building blocks of zinc oxide NPs biosynthesized by *Spirulina platensis* [42].

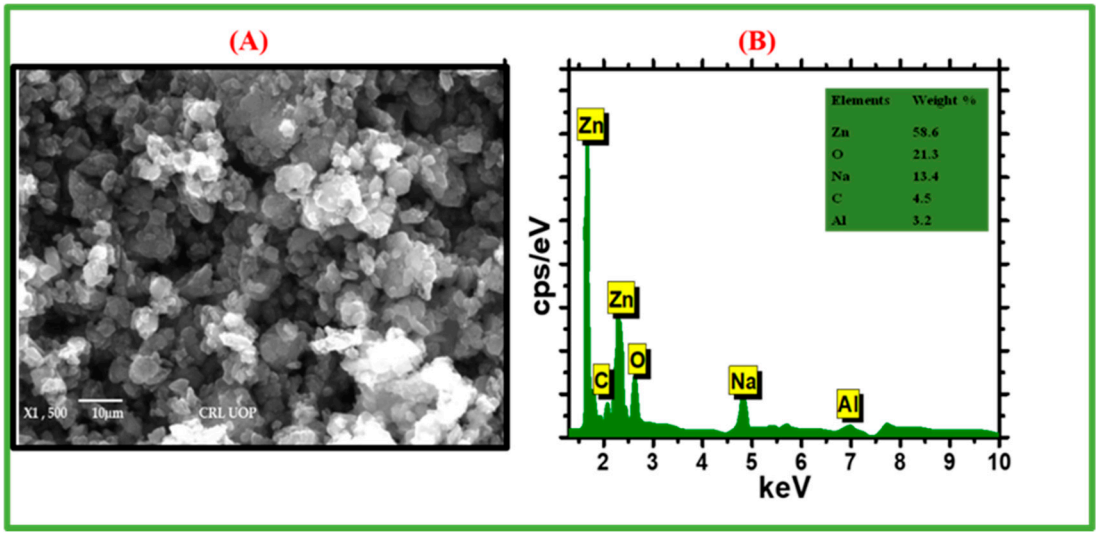


Figure 3. SEM and EDX images of green-synthesized zinc oxide NPs. (**A**) SEM image; (**B**) EDX spectrum.

2.1.4. XRD Pattern

The XRD pattern of biosynthesized zinc oxide nanoparticles is shown in Figure 4. In the XRD pattern, the broad peaks, with a clear broadening line, show the formation of the nanoscale zinc oxide particles. At 31.38, 34.03, 35.86, 47.18, 56.33, 62.48, 67.66, and 68.93, the zinc oxide NPs corresponded to the (100), (002), (101), (102), (110), (103), (112), and (201) crystallographic planes, respectively. Remarkably, the XRD pattern of the biosynthesized nanoparticles resembles the hexagonal wurtzite structure of zinc oxide [43]. The pattern obtained matches the JCPDS card no. 00-033-0664. Furthermore, for the high-intensity peak in the (101) plane of the diffractogram, the Debye–Scherrer equation was used to calculate the crystalline size of the zinc oxide nanoparticles of ~28.21 nm each [44]. As a result, it was observed in the XRD pattern of the zinc oxide NPs that the natural resources used to synthesize the NPs may have had a greater impact on the size of the zinc oxide NPs than on their crystal structure [30,45].

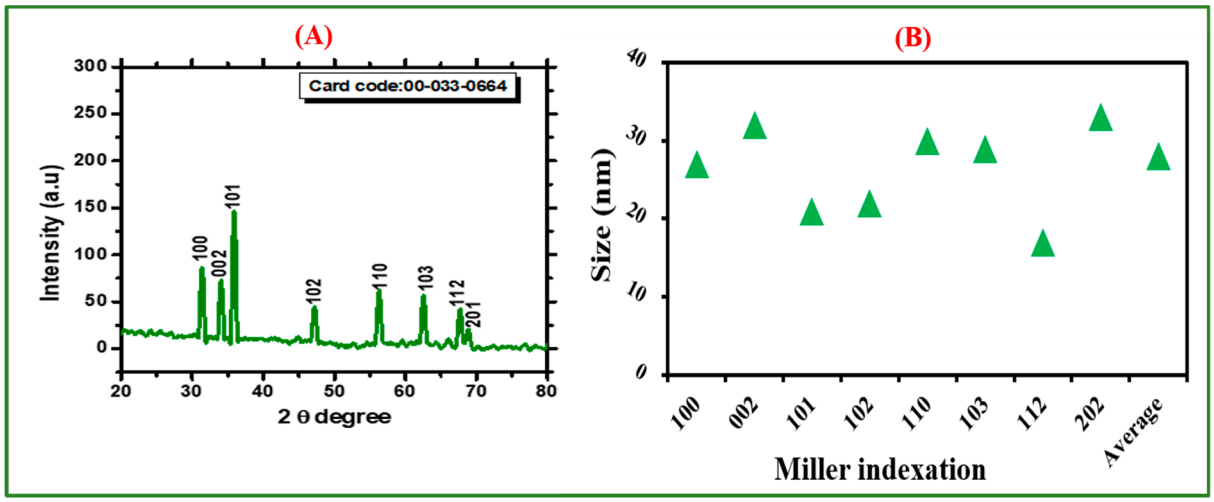


Figure 4. XRD pattern for biosynthesized zinc oxide NPs. (**A**) XRD pattern of *Nostoc* sp.-mediated zinc oxide; (**B**) size calculation using Debye–Scherrer equation.

Herein, we provide an overview of various reports of biological means of ZnONPs synthesis and discuss few of the landmark reports of the same. For the complete list of reports, please refer to Table 1.

Table 1. Comparative study of physical characterization of ZnONPs.

Source	Method	Chemical	Size	Shape	Surface Morphology	Crystal Nature	Reference
Sargassum muticum	Green synthesis	Zinc acetate dehydrate	42 nm	Hexagonal	Agglomerated	Crystalline	[46]
Cladophora Glomerata	Green synthesis	Zinc nitrate	30 nm	Spherical	Dispersed	Crystalline	[47]
Myristica Fragrans	Green synthesis	Zinc acetate dihydrate	41.23 nm	Semispherical shape	Agglomerated	Crystalline	[48]
Corriandrum Sativum	Chemical method	Zinc acetate dihydrate	81 nm	Flower shape	Agglomerated	Crystalline	[49]
Nostoc sp.	Green synthesis	Zinc acetate dihydrate	~28.21 nm	Hexagonal	Agglomerated	Crystalline	Current work

2.2. Biopotentials of Biogenic Nostoc sp. *Mediated Zinc Oxide Nanoparticles*

2.2.1. Analysis of Cytotoxic Assays

The most common method to determine the biological potency of a naturally occurring chemical is the brine shrimp lethality assay (BLSA) [50]. The cytotoxicity of the zinc oxide NPs was validated in a dose-dependent manner, and their IC50 value was determined as 11.15 µg mL^{-1}. The percentage mortality and dose-dependent behavior of the zinc oxide NPs are shown in Figure 5A. Our results from the brine shrimp mortality experiment are consistent with those of a zinc oxide NP assay that was previously reported [51].

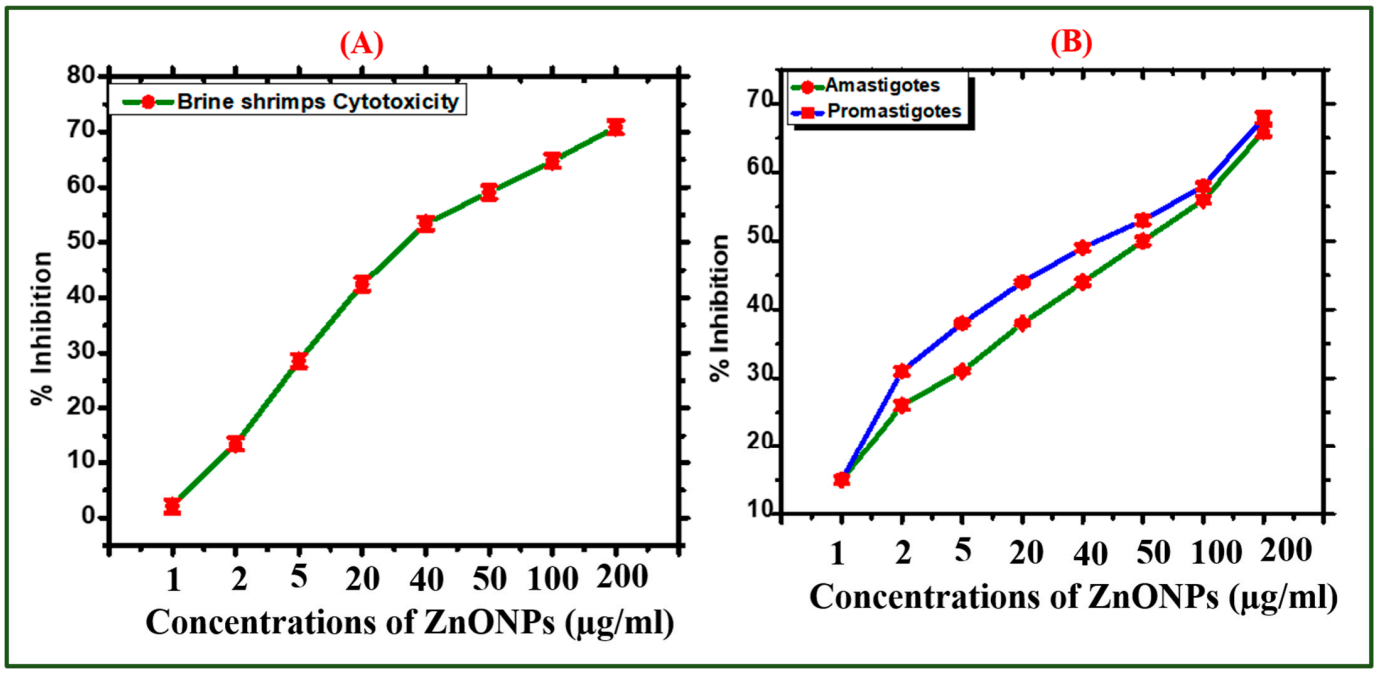


Figure 5. Analysis of cytotoxic activities. The data in these two figures represent the mean of three replications. (**A**) Cytotoxic capacity against brine shrimps; (**B**) antileishmanial activities of zinc oxide nanoparticles.

The antileishmanial drug antimonial is an effective drug for treating Leishmaniasis but has lost some of its therapeutic potential, as *Leishmania tropical* parasites have developed resistance to this. However, scholars are trying to look for an alternative strategy. Therefore, extensive research is required to create unique and potentially useful nanobiomaterials. Several nanomaterials have been reported to have anti-*L. tropica* activity [52]. However, biosynthesized zinc oxide nanoparticles have rarely been evaluated for their cytotoxic potential. In the present investigation, zinc oxide NPs have been used to treat *L. tropica* parasites at various concentrations from 1 to 200 µg.

Figure 5A shows the dose-dependent behavior of the antileishmanial potential of the ZnONPs. The ZnONPs showed promising activity against promastigotes and amastigotes of *L. tropica* (IC50: 14.02 µg/mL and 43.14 µg/mL, respectively). The current experiment results for the ZnONPs are comparable with those of a previous study [53].

2.2.2. Analysis of Antioxidant Assays

The antioxidant properties of the zinc oxide nanoparticles mediated by *Nostoc* sp. are depicted in Figure 6. The antioxidant capacities were evaluated in a concentration range of 1 to 200 µg/mL. To determine the presence of radical scavengers (antioxidant species) adsorbed on zinc (antioxidant species) adsorbed on the surfaces of the zinc oxide NPs, the free radical scavenging activity measured by 2, 2-diphenyl-1-picrylhydrazyl (DMSO) was utilized. Our DPPH results are comparable to those of a previously described study in which zinc oxide NPs were used. Their DPPH free radical scavenging activity

tests indicated a percentage free radical scavenging activity potential of 58.81% [30]. The maximum score for the total antioxidant capacity (TAC) of zinc oxide NPs in terms of ascorbic acid (AA) equivalent/mg was recorded as 51.43% at 200 µg mL^{-1}. The TAC activity is primarily used to determine the scavenging ability of tested chemicals toward reactive oxygen species. Our findings agreed with already published data [54]. In general, the antioxidant potential shows the availability of radical scavengers in the zinc oxide NPs, further promoting their stabilization [55].

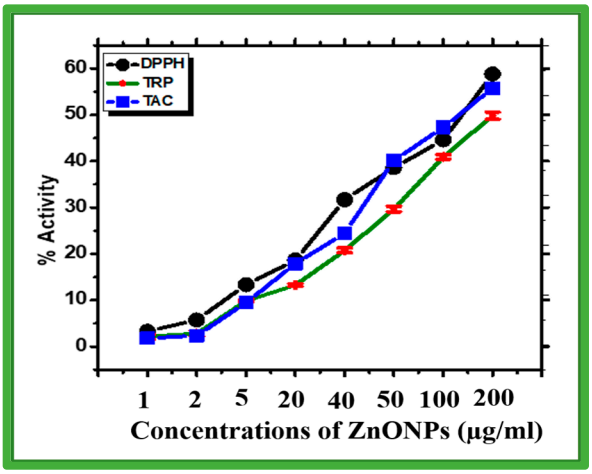


Figure 6. Antioxidant activities (DPPH, TRP, and TAC) of biosynthesized zinc oxide NPs. The data in this figure depict the mean of three replicates.

To further investigate the antioxidant species coated on the surface of biosynthesized NPs, a total reducing power (TRP) assay was designed. This assay was carried out to study the reductones, which play a significant role in antioxidant activity by adding hydrogen atoms and causing damage to the free radical chain [56]. The zinc oxide NPs made by biosynthesis displayed potential antioxidant action. With a decrease in the zinc oxide NP concentrations, the TRP also decreased. At maximum concentrations of 200 µg/mL, the highest TRP (49%) was noted. At 200 µg/mL, the zinc oxide nanoparticles revealed significant DPPH radical scavenging activity (58.81%). The information in Figure 6 leads to the conclusion that *Nostoc* cyanobacterial extracts can be used as a substrate for a variety of antioxidant compounds to reduce and stabilize zinc oxide NPs. For our zinc oxide NPs mediated by *Nostoc* sp., the antioxidant results are consistent with other findings in which zinc oxide NPs were used [51]. The differences and discrepancies compared to other studies may have been caused by several significant factors, such as the conditions of the experiment, the method used to create the nanoparticles, the cyanobacterial strain utilized, the strain component used, and the size of the nanoparticles, among others [30].

2.2.3. Biocompatibility Potential Assays

Human macrophages and RBCs were used to test the biocompatibility and toxicological effects of the zinc oxide NPs. Less than 2% of biological material is not hemolytic, while biological substances with a hemolytic activity greater than 5% are classified as hemolytic [57]. When a particular NP is hemolytic, it breaks down RBCs and releases hemoglobin as a by-product. Red blood cells (RBCs) were used in a hemolysis experiment to check the biosafety of the zinc oxide NPs. The zinc oxide NPs were used in different concentrations ranging from 200 to 1 µg/mL. Accordingly, the biosynthesized zinc oxide NPs were non-hemolytic at lower doses (2 µg/mL), slightly hemolytic at concentrations between 5 and 50 µg/mL, and hemolytic at concentrations above 50 µg/mL. These findings are consistent with previous observations of zinc oxide NPs [51]. The IC50 value of the zinc oxide NPs for human RBCs was determined as 433 µg/mL. The results of the current

study confirm that the biosynthesized zinc oxide NPs were non-hemolytic and considered biocompatible at low concentrations.

Human macrophages (HMs) were also used to confirm the biocompatibility assay. For this study, HMs were seeded in a 96-well plate and cultivated in an RPMI medium for 24 h for cell attachment. In addition, the cells were exposed to zinc oxide NPs at different concentrations (200 to 1 μg mL^{-1}). A dose-dependent response to the zinc oxide NPs was observed in the macrophages. The results show that the macrophages were inhibited by 35% of the zinc oxide NPs at concentrations of 200 μg mL^{-1}, which indicates the biosafety behavior of the biosynthesized zinc oxide NPs. Typically, macrophages have established inhibitors against reactive oxygen species (ROS) generated from an external source. According to researchers, lower production of reactive oxygen species is non-toxic to both macrophages and red blood cells unless the concentration rises above a certain limit, which is considered toxic to RBCs and macrophages [58]. The IC50 value was calculated to be >323 μg mL^{-1}. Figure 7B shows the results of the zinc oxide NP biocompatibility tests.

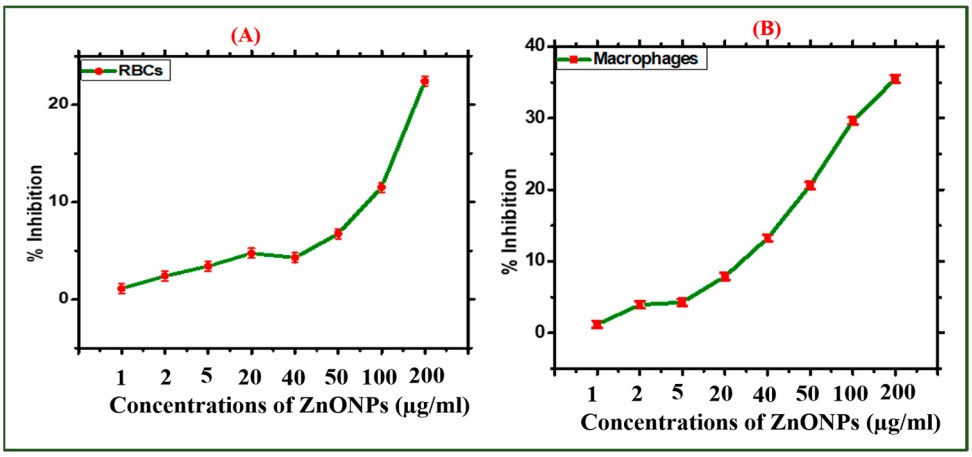


Figure 7. Biocompatibility potential assay of biosynthesized zinc oxide NPs. The data in all figures represent the mean (average) of three replicates. (**A**) Biocompatibility with human RBCs; (**B**) biocompatibility with human macrophages.

2.2.4. Analysis of Enzyme Inhibition Assays

The *Nostoc*-mediated zinc oxide NPs were evaluated for their protein kinase (PK) inhibition potential. Figure 8A shows the significant PK inhibitory capacity of the zinc oxide NPs at different doses between 37.5 and 1200 μg/mL. Our results show a moderate potential for the inhibition of PK. Furthermore, the zone of inhibition (ZOI) of 20.5 mm and the IC50 value of 400 μg/mL were determined. The ZOIs for the test sample were lower than those for surfactin (positive control). The results show that the cells were still viable at a relatively low concentration. The inhibition of protein kinase enzymes is thought to be a common target for the analysis of the anticancer potential of chemical substances. Tumor progression is caused by PK deregulation [59]. Our results indicate that zinc oxide NPs can inhibit the PK enzyme, suggesting that they should be investigated for the possibility of utilizing protein kinase inhibition to treat cancer. Our findings are consistent with previously published data [30].

In addition, the ability of the Nostoc-mediated zinc oxide NPs to inhibit α-amylase (AA) was evaluated. AA enzymes were subjected to various doses of the zinc oxide NPs (1200 to 18.75 μg/mL) to achieve this purpose. At a concentration of 1200 μg mL^{-1}, the zinc oxide NPs induced an increased percentage of inhibition (57.71%) (Figure 8B). On the other hand, the percentage of inhibition decreased as the zinc oxide NP concentrations decreased. The synthesized ZnONPs generally showed moderate enzyme inhibition potential, and our findings are similar to previously published data [54].

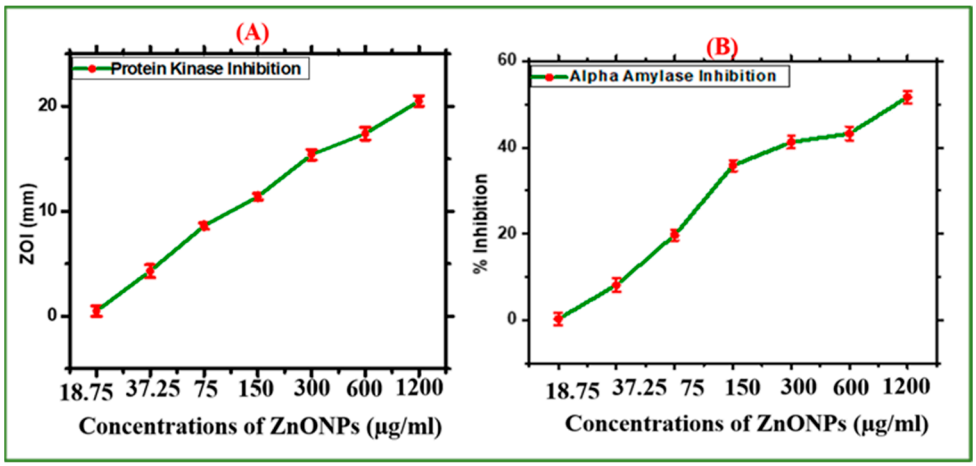


Figure 8. Enzyme inhibition potential of biosynthesized zinc oxide nanoparticles. The data in all figures represent the mean of three replicates. (**A**) Protein kinase inhibition; (**B**) α-amylase inhibition.

2.2.5. Antimicrobial Assays

Microbial inhibition has increased dramatically worldwide. Biogenic zinc oxide NPs were synthesized and used to combat multidrug-resistant superbugs. Zinc oxide NPs show remarkable fungicidal and bactericidal effects against multidrug-resistant infections. Various bacterial strains (BS), including *Staphylococcus aureus*, *Escherichia coli*, *Klebsiella pneumoniae*, and *coagulase-negative Staphylococcus* were used, and significant antibacterial activity results were obtained against the bacterial strains tested. It was observed that most BS were sensitive to the zinc oxide NPs. The minimum inhibitory concentration (MIC) values were recorded for different BS, including 50 µg/mL. Furthermore, it was investigated that *Staphylococcus aureus* was the least susceptible and *E. coli* was the most susceptible bacterial strain, with a minimum inhibition concentration (MIC) value of 50 µg mL^{-1}. Figure 9A,B illustrates the antibacterial potential of the zinc oxide NPs. No single concentrations of the zinc oxide NPs showed more potential than those of the positive control of kanamycin.

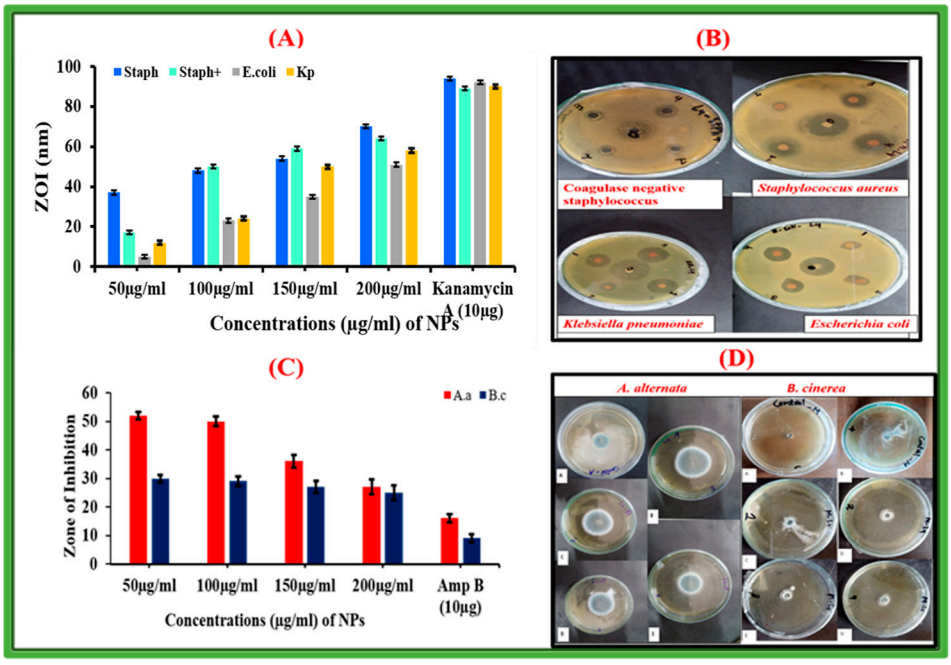


Figure 9. Antimicrobial assays. (**A**,**B**) Antibacterial assay of zinc oxide nanoparticles; (**C**,**D**) antifungal assay of zinc oxide nanoparticles.

The *Nostoc*-mediated zinc oxide NPs showed dose-dependent antimicrobial effects, and our findings are similar to previous studies on zinc oxide NPs using medicinal plants [60]. The bioactive compounds adsorbed onto the surface could be responsible for the significant antibacterial properties of zinc oxide NPs. In addition, research has shown that bactericidal and fungicidal effects can result from zinc oxide NP-produced ROS or microbial cell membrane perforations. Furthermore, these NPs can effectively penetrate microbial cell membranes through tiny holes, where they can disrupt the mineral balance and allow the leakage of intracellular proteins and enzymes, which will ultimately lead to cell growth suppression and cell death [61]. The antibacterial activity of zinc oxide nanoparticles has been the subject of extensive investigation, but little is known about their antifungal potential.

This study also evaluated the antifungal potential of the zinc oxide NPs against two different fungal strains; *Alternaria alternata* and *Botrytis cinerea*. The antifungal activity of the zinc oxide nanoparticles was investigated by treating fungal strains with various doses of zinc oxide NPs (50 to 200 µg/mL). The antifungal activity of the zinc oxide NPs is represented in Figure 9C,D. To determine the inhibitory potentials of the zinc oxide NPs, Amp-B served as a positive control. The results show a dose-dependent behavior. The least susceptible strain was *Botrytis cinerea*, while *Alternaria alternata* was the most susceptible strain [62].

3. Materials and Methods

3.1. Cyanobacterial Isolation Strain

All chemicals and solvents were obtained from Sigma-Aldrich. A water sample was collected from Gujar khan, District Rawalpindi, Pakistan. An isolated strain of *Nostoc* sp. was cultured and purified using blue-green algae medium (BG11) and incubated in a growth chamber at 25 °C with a 8/16 h photoperiod of dark/ light using cool white light with 3000 Lux. The colony emerged and was confirmed for purity; then it was preserved for further investigation. The morphological features, including shape, color, length, and width, were demonstrated using a light microscope. Taxonomic microscopy was achieved by following the methods of [63].

3.2. Cyanobacteria-Mediated Green Synthesis of Zinc Oxide NPs

3.2.1. Biomass Preparation

To generate biomass, *Nostoc* sp. was cultured in BG11 medium.

3.2.2. Green Synthesis of Zinc Oxide Nanoparticles

The logarithmic phase biomass of cyanobacteria was utilized for the green synthesis of zinc oxide NPs. The biomass of the cyanobacteria was harvested using a centrifuge. The cyanobacterial extract was prepared by adding 15 g of *Nostoc* sp. powder to 250 mL of distilled water. The zinc oxide NPs were synthesized as follows: 3 g of $Zn(CH_3COO)_2 \cdot 2H_2O$ was dissolved in 250 mL of distilled water; thereafter 98 mL of biomass filtrate was added. The mixture was then continuously stirred at 500 rpm for 2 h. To obtain NPs from zinc oxide in powder form, the resulting white precipitate was collected and dried in an oven for 4 h at 450 °C [64]. This powder was then used for further experiments. The study scheme of the biosynthesis, characterization, and biological activities of zinc oxide NPs is shown in Figure 10.

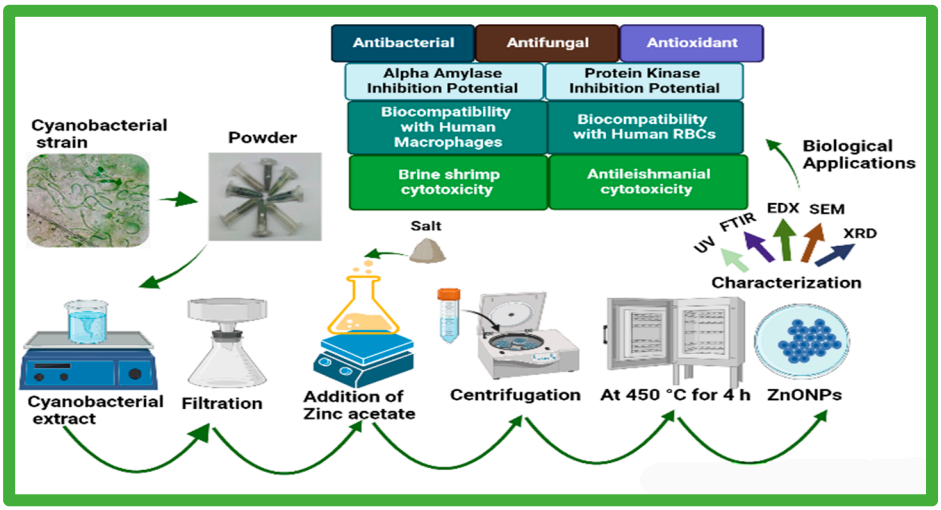


Figure 10. Study scheme showing the biosynthesis, characterization, and biological activities of zinc oxide NPs.

3.3. Characterization Techniques of Green-Synthesized Zinc Oxide NPs

3.3.1. UV-Vis Spectroscopy

The biosynthesis of the zinc oxide nanoparticles was investigated by changes in the colors of mixed solutions. The green synthesis of the zinc oxide nanoparticles in a colloidal solution was also examined by ultraviolet-visible spectroscopy (JENWAY 6305 Spectrophotometer, 230 V/50 Hz, Staffordshire, UK), as they revealed an intense absorption peak due to surface plasmon resonance. The changes in the color of the cyanobacterial extract/salt mixture were measured by spectrophotometry at wavelengths of 200–800 nm.

3.3.2. FTIR Analysis

Functional groups in the green-synthesized zinc oxide NPs were analyzed by FTIR spectra (JASCO FT-IR 4100 spectrometer, Hachioji, Tokyo, Japan). Potassium bromide (KBr) was combined with 0.2 µg of powdered zinc oxide NPs before loading them under high pressure onto a disk. FTIR spectra with 4.0 per centimeter, at wavelengths from 4000 cm^{-1} to 500 cm^{-1}, were used for functional group characterization.

3.3.3. XRD Analysis

The XRD spectrum (XRD, X'Pert Pro Philips, Dandong, China) was used to confirm the crystalline nature of the zinc oxide NPs with the following operating system: CuKα radiation—the 2θ angle ranged from 0° to 90°, λ = 1.540 Å. Additionally, the current was set to 30 mA, and the voltage was 40 Kv. The following Debye–Scherrer Equation (1) was used to calculate the average crystalline size of the NPs:

$$D = 0.9\lambda/\beta Cos\theta \quad (1)$$

where D is the average nanoparticle size, 0.9 is Scherrer's constant, λ is the X-ray wavelength, β is the full-width half-maximum, and θ is Bragg's angle.

3.3.4. SEM and EDX

To determine the surface properties and elemental composition of the green-synthesized zinc oxide NPs, SEM (JEOL JSM-6360LA, Tokyo, Japan) and EDX (EDX, Tokyo, Japan) were used [65].

3.4. Biological Applications of Nostoc-Mediated Green Synthesis of Zinc Oxide Nanoparticles

3.4.1. Brine Shrimp (BS) Cytotoxic Activity

The cytotoxic activity using brine shrimps was used to evaluate the cytotoxicity of biosynthesized zinc oxide nanoparticles [66]. *Artemia salina* eggs were incubated in seawater (3.8 g L^{-1}) for about 24–48 h at 30 °C under light conditions. Using Pasteur pipettes, 10 mature phototrophic nauplii were collected and placed in glass vials with zinc oxide NPs. Various concentrations (200 to 1 µg/mL) of zinc oxide NPs were used. The negative control consisted of vials of mature nauplii, vincristine sulfate, and seawater, and the positive control included mature nauplii flasks, seawater, and DMSO. The number of dead shrimps in each vial was counted after a 24-h incubation period. The graph pad program was used to calculate the IC50 values.

$$\text{Percentage Inhibition} = [\{1 - \frac{\text{sample}}{\text{control}}\}] \times 100 \quad (2)$$

3.4.2. Anti-Leishmanial Potential

In a subsequent evaluation of the cytotoxic potential of the zinc oxide NPs, *Leishmania tropica* (both amastigote and promastigote cultures) was used [67]. Using a Leishmania parasite culture, 10% FBS was added to MI99 medium. Zinc oxide NPs were administered to the Leishmania parasite at different concentrations from 1 to 200 µg mL^{-1} to evaluate their anti-Leishmania efficacy. The positive control of the experiment was amphotericin-B, and the negative control was DMSO. After that, the Leishmanial parasites were treated in 96-well plates with different concentrations of zinc oxide NPs and incubated in a carbon dioxide (5%) incubator at 24 °C for 72 h. The absorbance at a wavelength of 540 nm was measured, and IC50 values were calculated. Using the GraphPad program, the mean lethal concentration (IC50) and percentage inhibition were calculated using Equation (3):

$$\text{Percentage Inhibition} = [\{1 - \frac{\text{Absorbance of sample}}{\text{Absorbance of control}}\}] \times 100 \quad (3)$$

3.4.3. Antioxidant Assays

The spectrophotometric technique was utilized to assess the antioxidant capacity of zinc oxide nanoparticles. The working solution was prepared by adding 25 mL of methanol to 2.4 mg of free radicals (2.4 mg DPPH). Prior to assay, the antioxidant capacities of the zinc oxide NPs (1–200 µg/mL) at different concentrations were evaluated. For a negative control, DMSO was used, and ascorbic acid was used for a positive control. A sample of zinc oxide NPs (20 µL) and 180 µL of reagent solution were combined to make the 200 µL reaction mixtures [30]. The reaction mixture was kept in complete darkness for 2 h, and the absorbance of samples was measured at a wavelength of 517 nm. The ability of the zinc oxide NPs to eliminate free radicals was determined using Equation (4):

$$\text{Percentage DPPH Scavanging} = [\{1 - \frac{\text{ABs. sample}}{\text{ABs. control}}\}] \times 100 \quad (4)$$

Using the previously published phosphomolybdenum method, the total antioxidant capacity (TAC) was used to study the antioxidant capacity of the zinc oxide NPs [68]. The absorbance was measured at a wavelength of 695 nm, and the results are presented as the µg equivalents of ascorbic acid per milligram of test materials. DMSO served as a negative control, and AA (ascorbic acid) served as a positive control. Furthermore, the total reducing power (TRP) of the biosynthesized zinc oxide NPs was investigated using the potassium ferriccyanide method [69]. AA was used as a positive control and DMSO was used as a negative control. The absorbance of the mixed solutions was measured at a wavelength of 630 nm. The number of AA equivalents in milligrams (AAE/mg) was used to calculate the reducing power.

3.4.4. Biocompatibility with Human RBC

Using previously published techniques, the biocompatibility of the synthesized zinc oxide NPs was validated using human red blood cells [70]. First, 1 mL of fresh human RBCs were obtained and placed in an ethylene diamine tetraacetic acid (EDTA) falcon to avoid blood clotting during the hemolytic assay. The human blood cells were centrifuged for ten minutes at 12,000 rpm. The suspension of the red blood cells was prepared by mixing 200 µL of RBCs in 9.8 mL of phosphate-buffered saline (pH 7.2). Different concentrations (200 to 1 µg/mL) of zinc oxide NPs were mixed into 100 µL of the RBC suspension before being incubated at 35 °C for 1 h. Furthermore, the supernatant was separated by centrifugation at 12,000 rpm. The supernatant was then transferred to a 96-well plate. The hemoglobin release was investigated at 540 nm. In this experiment, for a negative control, DMSO was used, and for a positive control, Triton-X-100 was used. The results are expressed as the percentage hemolysis produced by various zinc oxide nanoparticle concentrations, and they were calculated using Equation (5):

$$\text{Percentage hemolysis } = [\frac{\text{Sample absorbance} - \text{Neg. control absorbance}}{\text{Pos. control absorbance} - \text{Neg. control absorbance}}] \times 100 \quad (5)$$

3.4.5. Biocompatibility with Human Macrophages (HMs)

The biocompatible nature of the biosynthesized zinc oxide NPs was also investigated using a previously described method [71]. The macrophages were cultured in Roswell Park Memorial Institute (RPMI) medium with 10% fetal bovine serum (FBS), 25 mM herpes, and antibiotics (pen–strep). Additionally, to promote cell adhesion, the macrophages were grown in 96-well plates and seeded with 5% CO_2 for 24 h. The macrophages were exposed to different biosynthesized zinc oxide NP concentrations (200 to 1 µg/mL) for 24 h. Equation (6) was used to determine the percentage inhibition:

$$\text{Percentage Inhibition} = [\{1 - \frac{\text{Absorbance of sample}}{\text{Absorbance of control}}\}] \times 100 \quad (6)$$

3.4.6. α-Amylase (AA) Inhibition Potential

Using a previously established technique, the potency of AA inhibition of the biosynthesized zinc oxide nanoparticles was evaluated [53]. To prepare the reaction mixture for the activity, 25 µL of AA, 10 µL of zinc oxide NPs, 15 µL of FBS, and 40 µL of starch solutions were combined. Then, 20 mL of iodine solutions and 90 mL of hydrochloric acid were mixed into the reaction solution containing all the compounds, and it was incubated at 50 °C for 30 min. In this experiment, ascorbose was taken as a positive control, and for a negative control, distilled water was used. The percentage inhibition was determined using Equation (7).

$$\text{Percentage inhibition } = [\frac{\text{Sample absorbance} - \text{Neg. control absorbance}}{\text{Pos. control absorbance} - \text{Neg.control absorbance}}] \times 100 \quad (7)$$

3.4.7. Protein Kinase Inhibitory Potential

A previously established method was used to investigate the potency of the zinc oxide nanoparticles to prevent protein kinase (PK) using the Streptomyces 85E strain [72]. In a sterile environment, the protein kinase inhibitory activity was performed. The SP4 minimal medium was used to generate Streptomyces lawns. In Petri dishes, the PK inhibitory potential of 10 µL of zinc oxide NPs placed on filter discs was evaluated. Surfactin was taken as a positive control, and for a negative control, DMSO was used. To achieve its growth, the Streptomyces 85E strain was cultured for 72 h at 30 °C. After 24 h, clear and bare zones surrounded the discs, showing that spore growth was restricted and mycelia were attached. Finally, the zone of inhibition (ZOI) was measured using Equation (8):

$$\text{Percentage inhibition } = [\frac{\text{Sample absorbance} - \text{Neg. control absorbance}}{\text{Pos. control absorbance} - \text{Neg. control absorbance}}] \times 100 \quad (8)$$

3.4.8. Antifungal Assays of ZnONPs

The antifungal activity of the ZnONPs was determined via the food poisoning method [73]. On PDA media, preserved cultures of fungi were cultivated for 72 h at 26.1 °C. Zinc oxide nanoparticles at various dose ranges (50–200 μg mL^{-1}) were mixed with the PDA medium for this investigation. A cork borer was used to insert a 4mm fungal inoculum disc into the center of the PDA plates. PDA without any nanoparticles was used as a positive control.

3.4.9. Antibacterial Assays of ZnONPs

An antibacterial assay of the zinc oxide nanoparticles was performed using a disc-diffusion technique [30]. The bacterial strains (BS) were subcultured in nutrient broth media and then incubated for twenty-four hours at 37 °C. To evaluate the antibacterial activity of the zinc oxide nanoparticles, an overnight culture of BS was plated on a prepared agar medium and left to dry for five minutes. The filter discs that were loaded with zinc oxide NPs at various concentrations (50–200 μg mL^{-1}) were then dried and left on the plate surface. The plate was incubated for 24 h at 37 °C while being checked for the zone of inhibition (ZOI). DMSO (5%) served as a negative control, and kanamycin-A served as a positive control.

4. Conclusions

In conclusion, our research has shown that a phytochemical-rich, toxin-free cyanobacterial *Nostoc* sp. extract can be used to rapidly and sustainably synthesize zinc oxide nanoparticles. The interactions of different elements in the cyanobacterial extract can lead to the biosynthesis of zinc oxide nanoparticles. The physical and chemical properties of biosynthesized zinc oxide nanoparticles were successfully investigated. The absorption band at a wavelength of 340 nm seen in the UV-vis spectroscopy confirms that zinc (Zn) metal ions were reduced to zinc oxide nanoparticles. The synthesized zinc oxide nanoparticles were about ~28 nm in size and spherical in shape. It is significant that this study also emphasized the numerous biological activities of zinc oxide NPs, showing that they have excellent antioxidant, biocompatible, and enzyme-inhibiting properties. Our findings show that the potency of zinc oxide nanoparticles indicate dose-dependent behavior. The results of the current study show that biosynthesized zinc oxide nanoparticles can be utilized as potential bio-safe candidates in a range of biological activities. To determine their nano-pharmacological importance in different bioactivities, more in vivo, in vitro, and mechanistic research in various animal models is needed in the future.

Author Contributions: L.A.M. developed the idea, conducted the experiments, analyzed the data, and wrote the manuscript. A.S.M. supervised the research project and provided laboratory facilities. M.K. and M.A.H.M. helped in writing and designing experiments. D.A.F. and R.M.M. helped in writing, editing, and revising the manuscript. M.A.H.M., R.W. and K.K. wrote some parts of the manuscript and software. All authors have read and agreed to the published version of the manuscript.

Funding: Funding was obtained from King Saud University, Researchers Supporting Project Number (RSP2023R190), King Saud University, Riyadh, Saudi Arabia.

Data Availability Statement: The data that support the findings of this study are available from the corresponding author upon request.

Acknowledgments: The authors acknowledge the financial support from King Saud University, Researchers Supporting Project Number (RSP2023R190), King Saud University, Riyadh, Saudi Arabia.

Conflicts of Interest: The authors declare no competing interests.

References

1. Singh, M.; Singh, H.; Prasad, S.; Gambhir, I.S. Nanotechnology in medicine and antibacterial effect of silver nanoparticles. *Dig. J. Nanomater. Biostruct.* **2008**, *3*, 115–122.
2. Pelaz, B.; Jaber, S.; De Aberasturi, D.J.; Wulf, V.; Aida, T.; de la Fuente, J.M.; Feldmann, J.; Gaub, H.E.; Josephson, L.; Kagan, C.R.; et al. The state of nanoparticle-based nanoscience and biotechnology: Progress, promises, and challenges. *ACS Publ.* **2012**, *6*, 8468–8483. [CrossRef]
3. Jianrong, C.; Yuqing, M.; Nongyue, H.; Xiaohua, W.; Sijiao, L. Nanotechnology and biosensors. *Biotechnol. Adv.* **2004**, *22*, 505–518. [CrossRef] [PubMed]
4. Zhang, X.; Guo, Q.; Cui, D. Recent advances in nanotechnology applied to biosensors. *Sensors* **2009**, *9*, 1033–1053. [CrossRef] [PubMed]
5. Chiou, J.W.; Kumar, K.K.; Jan, J.C.; Tsai, H.M.; Bao, C.W.; Pong, W.F.; Chien, F.Z.; Tsai, M.H.; Hong, I.H.; Klauser, R.; et al. Diameter dependence of the electronic structure of ZnO nanorods determined by X-ray absorption spectroscopy and scanning photoelectron microscopy. *Appl. Phys. Lett.* **2004**, *85*, 3220–3222. [CrossRef]
6. Rodgers, P. *Nanoscience and Technology: A Collection of Reviews from Nature Journals*; World Scientific: Singapore, 2009; 368p. [CrossRef]
7. Virkutyte, J.; Varma, R.S. Green synthesis of metal nanoparticles: Biodegradable polymers and enzymes in stabilization and surface functionalization. *Chem. Sci.* **2011**, *2*, 837–846. [CrossRef]
8. Nadagouda, M.N.; Varma, R.S. Green synthesis of silver and palladium nanoparticles at room temperature using coffee and tea extract. *Green Chem.* **2008**, *10*, 859–862. [CrossRef]
9. Darroudi, M.; Sabouri, Z.; Oskuee, R.K.; Zak, A.K.; Kargar, H.; Abd Hamid, M.H. Green chemistry approach for the synthesis of ZnO nanopowders and their cytotoxic effects. *Ceram. Int.* **2014**, *40*, 4827–4831. [CrossRef]
10. Iravani, S. Green synthesis of metal nanoparticles using plants. *Green Chem.* **2011**, *13*, 2638–2650. [CrossRef]
11. Behravan, M.; Panahi, A.H.; Naghizadeh, A.; Ziaee, M.; Mahdavi, R.; Mirzapour, A. Facile green synthesis of silver nanoparticles using *Berberis vulgaris* leaf and root aqueous extract and its antibacterial activity. *Int. J. Biol. Macromol.* **2019**, *124*, 148–154. [CrossRef]
12. Rajiv, P.; Rajeshwari, S.; Venckatesh, R. Bio-Fabrication of zinc oxide nanoparticles using leaf extract of *Parthenium hysterophorus* L. and its size-dependent antifungal activity against plant fungal pathogens. *Spectrochim. Acta Part A Mol. Biomol. Spectrosc.* **2013**, *112*, 384–387. [CrossRef]
13. Shinde, S.S. Antimicrobial activity of ZnO nanoparticles against pathogenic bacteria and fungi. *JSM Nanotechnol. Nanomed.* **2015**, *11*, 1033.
14. Moodley, J.S.; Krishna, S.B.; Pillay, K.; Govender, P. Green synthesis of silver nanoparticles from Moringa oleifera leaf extracts and its antimicrobial potential. *Adv. Nat. Sci. Nanosci. Nanotechnol.* **2018**, *9*, 015011. [CrossRef]
15. Chung, I.M.; Abdul Rahuman, A.; Marimuthu, S.; Vishnu Kirthi, A.; Anbarasan, K.; Padmini, P.; Rajakumar, G. Green synthesis of copper nanoparticles using *Eclipta prostrata* leaves extract and their antioxidant and cytotoxic activities. *Exp. Ther. Med.* **2017**, *14*, 18–24. [PubMed]
16. Suresh, J.; Pradheesh, G.; Alexramani, V.; Sundrarajan, M.; Hong, S.I. Green synthesis and characterization of zinc oxide nanoparticle using insulin plant (*Costus pictus D. Don*) and investigation of its antimicrobial as well as anticancer activities. *Adv. Nat. Sci. Nanosci. Nanotechnol.* **2018**, *9*, 015008. [CrossRef]
17. Mitra, S.; Patra, P.; Pradhan, S.; Debnath, N.; Dey, K.K.; Sarkar, S.; Chattopadhyay, D.; Goswami, A. Microwave synthesis of ZnO@mSiO_2 for detailed antifungal mode of action study: Understanding the insights into oxidative stress. *J. Colloid Interface Sci.* **2015**, *444*, 97–108. [CrossRef]
18. Yuvakkumar, R.; Suresh, J.; Saravanakumar, B.; Nathanael, A.J.; Hong, S.I.; Rajendran, V. Rambutan peels promoted biomimetic synthesis of bioinspired zinc oxide nanochains for biomedical applications. *Spectrochim. Acta Part A Mol. Biomol. Spectrosc.* **2015**, *137*, 250–258. [CrossRef]
19. Sabir, S.; Arshad, M.; Chaudhari, S.K. Zinc oxide nanoparticles for revolutionizing agriculture: Synthesis and applications. *Sci. World J.* **2014**, *2014*, 925494. [CrossRef]
20. Chaudhuri, S.K.; Malodia, L. Biosynthesis of zinc oxide nanoparticles using leaf extract of Calotropis gigantea: Characterization and its evaluation on tree seedling growth in nursery stage. *Appl. Nanosci.* **2017**, *7*, 501–512. [CrossRef]
21. Ebadi, M.; Zolfaghari, M.R.; Aghaei, S.S.; Zargar, M.; Shafiei, M.; Zahiri, H.S.; Noghabi, K.A. A bio-inspired strategy for the synthesis of zinc oxide nanoparticles (ZnO NPs) using the cell extract of cyanobacterium *Nostoc* sp. EA03: From biological function to toxicity evaluation. *RSC Adv.* **2019**, *9*, 23508–23525. [CrossRef]
22. Rastogi, R.P.; Sinha, R.P. Biotechnological and industrial significance of cyanobacterial secondary metabolites. *Biotechnol. Adv.* **2009**, *27*, 521–539. [CrossRef]
23. Correa, D.F.; Beyer, H.L.; Possingham, H.P.; Thomas-Hall, S.R.; Schenk, P.M. Biodiversity impacts of bioenergy production: Microalgae vs. first generation biofuels. *Renew. Sustain. Energy Rev.* **2017**, *74*, 1131–1146. [CrossRef]
24. Hamouda, R.A.; Hussein, M.H.; Abo-Elmagd, R.A.; Bawazir, S.S. Synthesis and biological characterization of silver nanoparticles derived from the cyanobacterium *Oscillatoria limnetica*. *Sci. Rep.* **2019**, *9*, 13071. [CrossRef] [PubMed]

25. El-Belely, E.F.; Farag, M.M.; Said, H.; Amin, A.S.; Azab, E.; Gobouri, A.A.; Fouda, A. Green synthesis of zinc oxide nanoparticles (ZnO-NPs) using *Arthrospira platensis* (Class: Cyanophyceae) and evaluation of their biomedical activities. *Nanomaterials* **2021**, *11*, 95. [CrossRef]
26. Ramesh, A.M.; Gangadhar, A.; Chikkamadaiah, M.; Shivanna, S. Antioxidant and photocatalytic properties of zinc oxide nanoparticles phyto-fabricated using the aqueous leaf extract of *Sida acuta*. *Green Process. Synth.* **2022**, *11*, 857–867. [CrossRef]
27. Pillai, A.M.; Sivasankarapillai, V.S.; Rahdar, A.; Joseph, J.; Sadeghfar, F.; Rajesh, K.; Kyzas, G.Z. Green synthesis and characterization of zinc oxide nanoparticles with antibacterial and antifungal activity. *J. Mol. Struct.* **2020**, *1211*, 128107. [CrossRef]
28. Gunalan, S.; Sivaraj, R.; Rajendran, V. Green synthesized ZnO nanoparticles against bacterial and fungal pathogens. *Prog. Nat. Sci. Mater. Int.* **2012**, *22*, 693–700. [CrossRef]
29. Morsy, F.M.; Nafady, N.A.; Abd-Alla, M.H.; Elhady, D.A. Green synthesis of silver nanoparticles by water soluble fraction of the extracellular polysaccharides/matrix of the cyanobacterium *Nostoc commune* and its application as a potent fungal surface sterilizing agent of seed crops. *Int. J. Microbiol.* **2014**, *2*, 36–43. [CrossRef]
30. Fatim, H.; Khan, K.; Zia, M.; Ur-Rehman, T.; Mirza, B.; Haq, I.U. Extraction optimization of medicinally important metabolites from *Datura innoxia* Mill.: An in vitro biological and phytochemical investigation. *BMC Complement. Altern. Med.* **2015**, *15*, 376. [CrossRef]
31. Abbasi, B.A.; Iqbal, J.; Ahmad, R.; Zia, L.; Kanwal, S.; Mahmood, T.; Wang, C.; Chen, J.T. Bioactivities of *Geranium wallichianum* leaf extracts conjugated with zinc oxide nanoparticles. *Biomolecules* **2019**, *10*, 38. [CrossRef]
32. Hamza, M.F.; Wei, Y.; Benettayeb, A.; Wang, X.; Guibal, E. Efficient removal of uranium, cadmium and mercury from aqueous solutions using grafted hydrazide-micro-magnetite chitosan derivative. *J. Mater. Sci.* **2020**, *55*, 4193–4212. [CrossRef]
33. Khalafi, T.; Buazar, F.; Ghanemi, K. Phycosynthesis and enhanced photocatalytic activity of zinc oxide nanoparticles toward organosulfur pollutants. *Sci. Rep.* **2019**, *9*, 6866. [CrossRef] [PubMed]
34. Duygu, D.Y.; Udoh, A.U.; Ozer, T.B.; Akbulut, A.; Erkaya, I.A.; Yildiz, K.; Guler, D. Fourier transform infrared (FTIR) spectroscopy for identification of *Chlorella vulgaris* Beijerinck 1890 and *Scenedesmus obliquus* (Turpin) Kützing 1833. *Afr. J. Biotechnol.* **2012**, *11*, 3817–3824.
35. Hamza, M.F.; Roux, J.-C.; Guibal, E. Uranium and europium sorption on amidoxime-functionalized magnetic chitosan microparticles. *Chem. Eng. J.* **2018**, *344*, 124–137. [CrossRef]
36. Buazar, F.; Bavi, M.; Kroushawi, F.; Halvani, M.; Khaledi-Nasab, A.; Hossieni, S.A. Potato extract as reducing agent and stabiliser in a facile green one-step synthesis of ZnO nanoparticles. *J. Exp. Nanosci.* **2016**, *11*, 175–184. [CrossRef]
37. Nagarajan, S.; Arumugam Kuppusamy, K. Extracellular synthesis of zinc oxide nanoparticle using seaweeds of gulf of Mannar, India. *J. Nanobiotechnol.* **2013**, *11*, 39. [CrossRef]
38. Zhang, G.; Shen, X.; Yang, Y. Facile synthesis of monodisperse porous ZnO spheres by a soluble starch-assisted method and their photocatalytic activity. *J. Phys. Chem. C* **2011**, *115*, 7145–7152. [CrossRef]
39. Singh, J.; Kaur, S.; Kaur, G.; Basu, S.; Rawat, M. Biogenic ZnO nanoparticles: A study of blueshift of optical band gap and photocatalytic degradation of reactive yellow 186 dye under direct sunlight. *Green Process. Synth.* **2019**, *8*, 272–280. [CrossRef]
40. Fakhari, S.; Jamzad, M.; Kabiri Fard, H. Green synthesis of zinc oxide nanoparticles: A comparison. *Green Chem. Lett. Rev.* **2019**, *12*, 19–24. [CrossRef]
41. Hosny, M.; Fawzy, M.; Eltaweil, A.S. Green synthesis of bimetallic Ag/ZnO@Biohar nanocomposite for photocatalytic degradation of tetracycline, antibacterial and antioxidant activities. *Sci. Rep.* **2022**, *12*, 7316. [CrossRef]
42. Fouda, A.; Hassan, S.E.; Saied, E.; Azab, M.S. An eco-friendly approach to textile and tannery wastewater treatment using maghemite nanoparticles (γ-Fe_2O_3-NPs) fabricated by *Penicillium expansum* strain (Kw). *J. Environ. Chem. Eng.* **2021**, *9*, 104693.
43. Djearamane, S.; Lim, Y.M.; Wong, L.S.; Lee, P.F. Cytotoxic effects of zinc oxide nanoparticles on cyanobacterium *Spirulina* (*Arthrospira*) *platensis*. *PeerJ* **2018**, *6*, e4682.
44. Li, Z.; Zhou, Z.; Yun, G.; Shi, K.; Lv, X.; Yang, B. High-performance solid-state supercapacitors based on graphene-ZnO hybrid nanocomposites. *Nanoscale Res. Lett.* **2013**, *8*, 473.
45. Jaber, B.; Laânab, L. One step synthesis of ZnO nanoparticles in free organic medium: Structural and optical characterizations. *Mater. Sci. Semicond. Process.* **2014**, *27*, 446–451.
46. Azizi, S.; Ahmad, M.B.; Namvar, F.; Mohamad, R. Green biosynthesis and characterization of zinc oxide nanoparticles using brown marine macroalga *Sargassum muticum* aqueous extract. *Mater. Lett.* **2014**, *116*, 275–277.
47. Abdulwahid, K.E.; Dwaish, A.S.; Dakhil, O.A. Green synthesis and characterization of zinc oxide nanoparticles from *Cladophora glomerata* and its antifungal activity against some fungal isolates. *Plant Arch.* **2019**, *19*, 3527–3532.
48. Faisal, S.; Jan, H.; Shah, S.A.; Shah, S.; Khan, A.; Akbar, M.T.; Rizwan, M.; Jan, F.; Wajidullah Akhtar, N.; Khattak, A. Green synthesis of zinc oxide (ZnO) nanoparticles using aqueous fruit extracts of *Myristica fragrans*: Their characterizations and biological and environmental applications. *ACS Omega* **2021**, *6*, 9709–9722.
49. Gnanasangeetha, D.; Sarala Thambavani, D. One pot synthesis of zinc oxide nanoparticles via chemical and green method. *Res. J. Mater. Sci.* **2013**, *2320*, 6055.
50. Gao, Y.; Xu, D.; Ren, D.; Zeng, K.; Wu, X. Green synthesis of zinc oxide nanoparticles using *Citrus sinensis* peel extract and application to strawberry preservation: A comparison study. *Food Sci. Technol.* **2020**, *126*, 109297.
51. Chanda, S.; Baravalia, Y. Brine shrimp cytotoxicity of *Caesalpinia pulcherrima* aerial parts, antimicrobial activity and characterisation of isolated active fractions. *Nat. Prod. Res.* **2011**, *25*, 1955–1964.

52. Khalil, A.T.; Ovais, M.; Ullah, I.; Ali, M.; Shinwari, Z.K.; Hassan, D.; Maaza, M. *Sageretia thea* (Osbeck.) modulated biosynthesis of NiO nanoparticles and their in vitro pharmacognostic, antioxidant and cytotoxic potential. *Artif. Cells Nanomed. Biotechnol.* **2018**, *46*, 838–852. [CrossRef]
53. Rajendran, K.; Karunagaran, V.; Mahanty, B.; Sen, S. Biosynthesis of hematite nanoparticles and its cytotoxic effect on HepG2 cancer cells. *Int. J. Biol. Macromol.* **2015**, *74*, 376–381. [CrossRef]
54. Iqbal, J.; Abbasi, B.A.; Mahmood, T.; Hameed, S.; Munir, A.; Kanwal, S. Green synthesis and characterizations of Nickel oxide nanoparticles using leaf extract of *Rhamnus virgata* and their potential biological applications. *Appl. Organomet. Chem.* **2019**, *33*, e4950. [CrossRef]
55. Mittal, A.K.; Chisti, Y.; Banerjee, U.C. Synthesis of metallic nanoparticles using plant extracts. *Biotechnol. Adv.* **2013**, *31*, 346–356. [CrossRef]
56. Ul-Haq, I.; Ullah, N.; Bibi, G.; Kanwal, S.; Ahmad, M.S.; Mirza, B. Antioxidant and cytotoxic activities and phytochemical analysis *Euphorbia wallichii* root extract and its fractions. *Iran. J. Pharm. Res. (IJPR)* **2012**, *11*, 241–249.
57. Dobrovolskaia, M.A.; Clogston, J.D.; Neun, B.W.; Hall, J.B.; Patri, A.K.; McNeil, S.E. Method for analysis of nanoparticle hemolytic properties in vitro. *Nano Lett.* **2008**, *8*, 2180–2187. [CrossRef]
58. Prach, M.; Stone, V.; Proudfoot, L. Zinc oxide nanoparticles and monocytes: Impact of size, charge and solubility on activation status. *Toxicol. Appl. Pharmacol.* **2013**, *266*, 19–26. [CrossRef]
59. Waters, B.; Saxena, G.; Wanggui, Y.; Kau, D.; Wrigley, S.; Stokes, R.; Davies, J. Identifying protein kinase inhibitors using an assay based on inhibition of aerial hyphae formation in Streptomyces. *J. Antibiot.* **2002**, *55*, 407–416. [CrossRef]
60. Yao, G.; Sebisubi, F.M.; Voo, L.Y.; Ho, C.C.; Tan, G.T.; Chang, L.C. Citrinin derivatives from the soil filamentous fungus *Penicillium* sp. H9318. *J. Braz. Chem. Soc.* **2011**, *22*, 1125–1129. [CrossRef]
61. Mahdavi, B.; Saneei, S.; Qorbani, M.; Zhaleh, M.; Zangeneh, A.; Zangeneh, M.M.; Pirabbasi, E.; Abbasi, N.; Ghaneialvar, H. *Ziziphora clinopodioides* Lam leaves aqueous extract mediated synthesis of zinc nanoparticles and their antibacterial, antifungal, cytotoxicity, antioxidant, and cutaneous wound healing properties under in vitro and in vivo conditions. *Appl. Organomet. Chem.* **2019**, *33*, e5164. [CrossRef]
62. Li, Y.; Zhang, W.; Niu, J.; Chen, Y. Mechanism of photogenerated reactive oxygen species and correlation with the antibacterial properties of engineered metal-oxide nanoparticles. *ACS Nano* **2012**, *6*, 5164–5173. [CrossRef]
63. Edlund, M.B. *Freshwater Algae of North America—Ecology and Classification*; Academic Press: Cambridge, MA, USA, 2003. [CrossRef]
64. Fouda, A.; Eid, A.M.; Elsaied, A.; El-Belely, E.F.; Barghoth, M.G.; Azab, E.; Gobouri, A.A.; Hassan, S.E. Plant growth-promoting endophytic bacterial community inhabiting the leaves of *Pulicaria incisa* (Lam.) DC inherent to arid regions. *Plants* **2021**, *10*, 76. [CrossRef]
65. Shaheen, T.I.; Fouda, A. Green approach for one-pot synthesis of silver nanorod using cellulose nanocrystal and their cytotoxicity and antibacterial assessment. *Int. J. Biol. Macromol.* **2018**, *106*, 784–792. [CrossRef] [PubMed]
66. Supraja, N.; Prasad, T.N.V.K.V.; Gandhi, A.D.; Anbumani, D.; Kavitha, P.; Babujanarthanam, R. Synthesis, characterization and evaluation of antimicrobial efficacy and brine shrimp lethality assay of *Alstonia scholaris* stem bark extract mediated ZnONPs. *Biochem. Biophys. Rep.* **2018**, *14*, 69–77. [CrossRef] [PubMed]
67. Abbasi, B.A.; Iqbal, J.; Mahmood, T.; Khalil, A.T.; Ali, B.; Kanwal, S.; Shah, S.A.; Ahmad, R. Role of dietary phytochemicals in modulation of miRNA expression: Natural swords combating breast cancer. *Asian Pac. J. Trop. Med.* **2018**, *11*, 501–509.
68. Bharadwaj, K.K.; Rabha, B.; Pati, S.; Choudhury, B.K.; Sarkar, T.; Gogoi, S.K.; Kakati, N.; Baishya, D.; Kari, Z.A.; Edinur, H.A. Antioxidant and anticancer activities of green synthesized silver nanoparticles using aqueous extract of tubers of *Pueraria tuberosa*. *Artif. Cells Nanomed. Biotechnol.* **2018**, *46*, S71–S85.
69. Baqi, A.; Tareen, R.B.; Mengal, A.; Khan, N.; Behlil, F.; Achakzai, A.K.; Faheem, M. Determination of antioxidants in two medicinally important plants, *Haloxylon griffithii* and *Convolvulus leiocalycinus*, of Balochistan. *Pure Appl. Biol.* **2018**, *7*, 296–308. [CrossRef]
70. Malagoli, D. A full-length protocol to test hemolytic activity of palytoxin on human erythrocytes. *Invertebr. Surviv. J.* **2007**, *4*, 92–94.
71. De Almeida, M.C.; Silva, A.C.; Barral, A.; Barral Netto, M. A simple method for human peripheral blood monocyte isolation. *Mem. Inst. Oswaldo Cruz* **2000**, *95*, 221–223. [CrossRef]
72. Iqbal, J.; Abbasi, B.A.; Mahmood, T.; Kanwal, S.; Ahmad, R.; Ashraf, M. Plant-extract mediated green approach for the synthesis of ZnONPs: Characterization and evaluation of cytotoxic, antimicrobial and antioxidant potentials. *J. Mol. Struct.* **2019**, *1189*, 315–327. [CrossRef]
73. Ahmed, J.; Ali, M.; Sheikh, H.M.; Al-Kattan, M.O.; Haroon, U.; Safaeishakib, M.; Akbar, M.; Kamal, A.; Zubair, M.S.; Munis, M.F. Biocontrol of Fruit Rot of Litchi chinensis Using Zinc Oxide Nanoparticles Synthesized in *Azadirachta indica*. *Micromachines* **2022**, *13*, 1461. [CrossRef]

Disclaimer/Publisher's Note: The statements, opinions and data contained in all publications are solely those of the individual author(s) and contributor(s) and not of MDPI and/or the editor(s). MDPI and/or the editor(s) disclaim responsibility for any injury to people or property resulting from any ideas, methods, instructions or products referred to in the content.